



OPEN

SUBJECT AREAS:

POLYMERS

PLANT BIOTECHNOLOGY

Received

12 October 2014

Accepted

10 December 2014

Published

13 January 2015

Correspondence and requests for materials should be addressed to K.N. (keiji.numata@riken.jp)

Gene introduction into the mitochondria of *Arabidopsis thaliana* via peptide-based carriers

Jo-Ann Chuah¹, Takeshi Yoshizumi², Yutaka Kodama³ & Keiji Numata¹

¹Enzyme Research Team, Biomass Engineering Program Cooperation Division, Center for Sustainable Resource Science, RIKEN, 2-1 Hirotsawa, Wako-shi, Saitama 351-0198, Japan, ²Institute for Advanced Biosciences, Keio University, 403-1 Nipponkoku, Daihoji, Tsuruoka, Yamagata 997-0017, Japan, ³Center for Bioscience Research and Education, Utsunomiya University, Tochigi 321-8505, Japan.

Available methods in plant genetic transformation are nuclear and plastid transformations because similar procedures have not yet been established for the mitochondria. The double membrane and small size of the organelle, in addition to its large population in cells, are major obstacles in mitochondrial transfection. Here we report the intracellular delivery of exogenous DNA localized to the mitochondria of *Arabidopsis thaliana* using a combination of mitochondria-targeting peptide and cell-penetrating peptide. Low concentrations of peptides were sufficient to deliver DNA into the mitochondria and expression of imported DNA reached detectable levels within a short incubation period (12 h). We found that electrostatic interaction with the cell membrane is not a critical factor for complex internalization, instead, improved intracellular penetration of mitochondria-targeted complexes significantly enhanced gene transfer efficiency. Our results delineate a simple and effective peptide-based method, as a starting point for the development of more sophisticated plant mitochondrial transfection strategies.

In plants, the mitochondrion plays the fundamental role of energy generation and is involved in the detection of developmental signals, biotic and abiotic stresses¹. The organelle also functions in reactive oxygen species induction and signaling, genome maintenance, respiration, and programmed cell death². Methods that enable access into the plant mitochondria thus offer exciting avenues for study and manipulation of these essential physiological and biochemical processes. The mitochondrion is also a prospective new target for genetic engineering of plants, as an alternative to modification of the nucleus or plastids. Simultaneous expression of transgenes in different organelles may occur via the transformed mitochondria through interorganellar communication pathways within the cell^{3,4}, as an effective approach to metabolically engineer the plant cell factory. Plant cells have shown great potential as hosts for the production of valuable medicinal compounds, pharmaceutically important secondary metabolites, recombinant proteins, flavors, fragrances, and colorants – none of which can be produced by microbial cells or chemical synthesis⁵.

Although the ability to introduce exogenous genes into plant mitochondria has wide biotechnological and fundamental significance, this complex organelle could not be transformed in whole plants with currently existing methodologies⁶. The double membrane and small size of the organelle are major obstacles in mitochondrial transfection⁷. To date, mitochondrial transformation has only been achieved using isolated plant mitochondria (by electrotransformation⁸ or natural competence⁹), as well as in yeast^{10,11} and *Chlamydomonas*^{12,13} (both by biolistic method), however this milestone has not yet been accomplished for any vascular plant. Mitochondrial transformation by microparticle bombardment^{10–13} is disadvantageous in terms of low frequency of transformant recovery. The lack of selectable markers for mitochondrial transformation adds to the challenge.

Peptides are a highly versatile and efficient class of transporters with the ability to translocate the cellular membrane and/or organellar membranes, and their potential use as gene delivery vectors has been substantiated in numerous studies^{14–20}. Taking advantage of their innate nature, we aimed to develop a peptide-based carrier for delivery of genes specifically to the mitochondria in plants, where the peptide sequences were rationally determined based on the vast range of available information from associated studies in the past.

Results

Delivering plasmid DNA using the designed mitochondria-targeting peptide. The mitochondria-targeting component consists of the first 12 amino acids of the presequence belonging to the yeast cytochrome *c* oxidase



subunit IV that was capable of directing attached mouse cytosolic dihydrofolate reductase into the yeast mitochondrial matrix, both *in vitro* and *in vivo*²¹. The mitochondria-targeting dodecapeptide (hereafter referred to as MTP) was fused to a polycationic copolymer of alternating histidine and lysine residues (Fig. 1a). Polycations comprising histidine and lysine residues have proven to be beneficial in increasing cell transfection efficiencies^{16,17,20} and should, as we anticipate, help to facilitate electrostatic complexation of the resultant fusion peptide (designated MTP_{KH}) and the polyanionic plasmid DNA (pDNA).

The stability of complexes formed upon binding of MTP and MTP_{KH}, individually, with pDNA was investigated by an electrophoretic mobility shift assay (Fig. 1b). MTP exhibited weak pDNA binding and caused only a slight retention in pDNA shift even at a high N/P (defined as the number of amine groups from the peptide/the number of phosphate groups from pDNA) ratio of 100. The addition of polycations to MTP, particularly at higher concentrations (N/P 2 and above), proved to be essential in stabilizing the formed complexes. MTP_{KH} severely impaired pDNA mobility at N/P 2 and complex stability continued to increase with N/P ratio until complete retardation of pDNA movement was attained at N/P 20.

We also examined the tendencies of MTP and MTP_{KH} to condense pDNA by an ethidium bromide (EtBr) exclusion assay, as pDNA condensation is required for receptor-mediated uptake of complexes²². The binding of peptide causes conformational changes to the pDNA, resulting in displacement of intercalated EtBr which subsequently quenches the fluorescence from the EtBr-pDNA complex. At each of the distinct N/P ratios (0.5, 2, 5, 20) used for complex preparation in this assay, MTP_{KH} quenched the fluorescence with better efficiency than MTP, and achieved nearly complete quenching (approximately 90%) at N/P 20 (Fig. 1c).

The size of particles formed using MTP were relatively large and independent of polycation concentration (Fig. 1d), coherent with its poor pDNA binding/compacting abilities. In contrast, MTP_{KH} enabled formation of more compact particles with hydrodynamic diameters averaging between 140 nm and 480 nm, which are compatible with the caveolae-mediated endocytic pathway^{23,24}. The surface charges of particles, which can contribute to cellular uptake^{15,23,25}, were subsequently characterized (Fig. 1e). The ζ -potential of MTP-pDNA complexes were negative at all N/P ratios, although decrease in negative charges were seen with increasing N/P ratio, whereas those of complexes formed using MTP_{KH} transitioned from negative (N/P 0.1 to 2) to positive (N/P 5 to 20).

Next, we proceeded to evaluate the functionality of the designed MTP_{KH} in mitochondria-targeted gene delivery. MTP_{KH}-pDNA complexes prepared at N/P ratios ranging from 0.1 to 20, as before, were infiltrated into the leaves of *Arabidopsis thaliana*, which serves as a model plant system. The pDNA harbors the gene encoding *Renilla* luciferase (RLuc) enzyme, which is expressed under the control of the mitochondrial-specific cyclooxygenase-2 (COX-2) promoter²⁶. Expression of the reporter gene in the mitochondrial compartment of leaves, sampled at intermittent time points, was quantitatively determined by an RLuc assay. Complexes prepared at N/P 0.5 demonstrated remarkable transfection ability, well surpassing the transfection levels mediated by complexes of the other N/P ratios, and this interesting observation was true for all incubation periods tested (Fig. 1f). In contrast, complexes formed using MTP or lysine-histidine copolymer (N/P 0.5) or naked pDNA, when delivered to leaves, mediated negligible levels of expression (Supplementary Fig. 1).

Secondary structures of MTP and MTP_{KH}, as well as their pDNA-bound versions (representative N/P ratio of 0.5, the most transfection-effective formulation), were therefore analysed by circular dichroism (CD) (Fig. 1g). MTP and MTP-pDNA showed either a random or low level of structuring. In contrast, the spectra of MTP_{KH} exhibited characteristic features of an α -helical structure (double

minima at 207 and 222 nm)²⁷ and the α -helicity was retained even upon complexation with pDNA.

Enhancing pDNA delivery by addition of a cell-penetrating peptide. The net negative surface charge of the MTP_{KH}-pDNA complex (N/P 0.5) was fortuitous as it inspired a strategy, which we discovered later, to significantly improve the performance of our designed pDNA carrier. By the same principle that enabled interaction between the negatively-charged pDNA molecule and positively-charged MTP_{KH}, we allowed new cell-penetrating components to electrostatically interact with negatively-charged MTP_{KH}-pDNA complexes at N/P 0.5. The cell-penetrating peptides used were: (i) the BP100 peptide (hereafter referred to as CPP) and (ii) the fusion of CPP to the same copolymer of alternating lysine and histidine residues as before (designated CPP_{KH}) (Fig. 2a). Both CPP and CPP_{KH} have displayed potential as efficient plant cell-penetrating tools^{14,17}.

The resultant CPP- or CPP_{KH}-MTP_{KH}-pDNA complexes were characterized biophysically and functionally, as done previously. Addition of CPP and CPP_{KH} further stabilized the MTP_{KH}-pDNA complexes and a gradual increment in stability was seen with increasing N/P ratio until complete charge neutralization occurred at N/P 100 for both peptides (Fig. 2b). CPP and CPP_{KH} also exhibited similar tendencies for pDNA condensation at each of the different N/P ratios (Fig. 2c). No apparent differences in average diameters were detected between complexes formed using CPP and CPP_{KH} at each N/P ratio, except when CPP was added at higher N/P ratios of 50 and 100, highly polydisperse particles were formed (Supplementary Table 1). Particle sizes were in the narrow range of 160–280 nm (Fig. 2d) and in terms of surface charge, ζ -potential values gradually transitioned from negative to positive for both CPP- and CPP_{KH}-based complexes (Fig. 2e).

The various formulations were used to transfect *A. thaliana* leaves, in a similar manner as with the MTP_{KH}-pDNA complexes, maintaining the 12 h incubation period that was previously determined to be sufficient for mitochondrial expression of the RLuc reporter gene. Results from evaluation by RLuc assay showed a marked increase in transfection levels, more than that of MTP_{KH}-pDNA complexes, only by supplementation of CPP at N/P 0.5 (Fig. 2f). These transfection-optimized complexes, formed by sequential mixing of MTP_{KH} and CPP (both at N/P 0.5) with pDNA, displayed a relatively uniform distribution in size when observed by scanning electron microscopy (SEM) (Supplementary Fig. 2). Through additional experiments, we found no/low levels of extramitochondrial RLuc gene expression (i.e. cytosolic expression) by the mitochondrial-specific COX-2 promoter (Supplementary Fig. 3). We also performed conformational analysis by CD and found that both CPP and CPP_{KH} were α -helical when bound to pDNA (Fig. 2g).

As a final step, the efficiency of our designed peptide-based carrier was verified by delivery of pDNA containing a gene that encodes another well-known reporter, the green fluorescent protein (GFP), also under the control of the same mitochondrial COX-2 promoter. For comparison, leaves were infiltrated with either naked pDNA, MTP_{KH}-pDNA or CPP-MTP_{KH}-pDNA, and mitochondrial expression of GFP was subsequently detected by Western blotting using an anti-GFP antibody. Of the three different formulations, only the CPP-MTP_{KH} combination mediated pDNA delivery and significant levels of GFP expression, as evident from the band corresponding to the size of 27 kDa GFP (Fig. 3a). Confocal laser scanning microscopy provided visual confirmation of GFP expression, localized in the mitochondria of epidermal cells of leaves transfected using the optimized peptide-pDNA formulation (MTP_{KH} and CPP at N/P 0.5 each) (Fig. 3b).

Discussion

We sought to understand the merits of the MTP_{KH}-pDNA complex (N/P 0.5) over other formulations in enabling efficient gene transfer

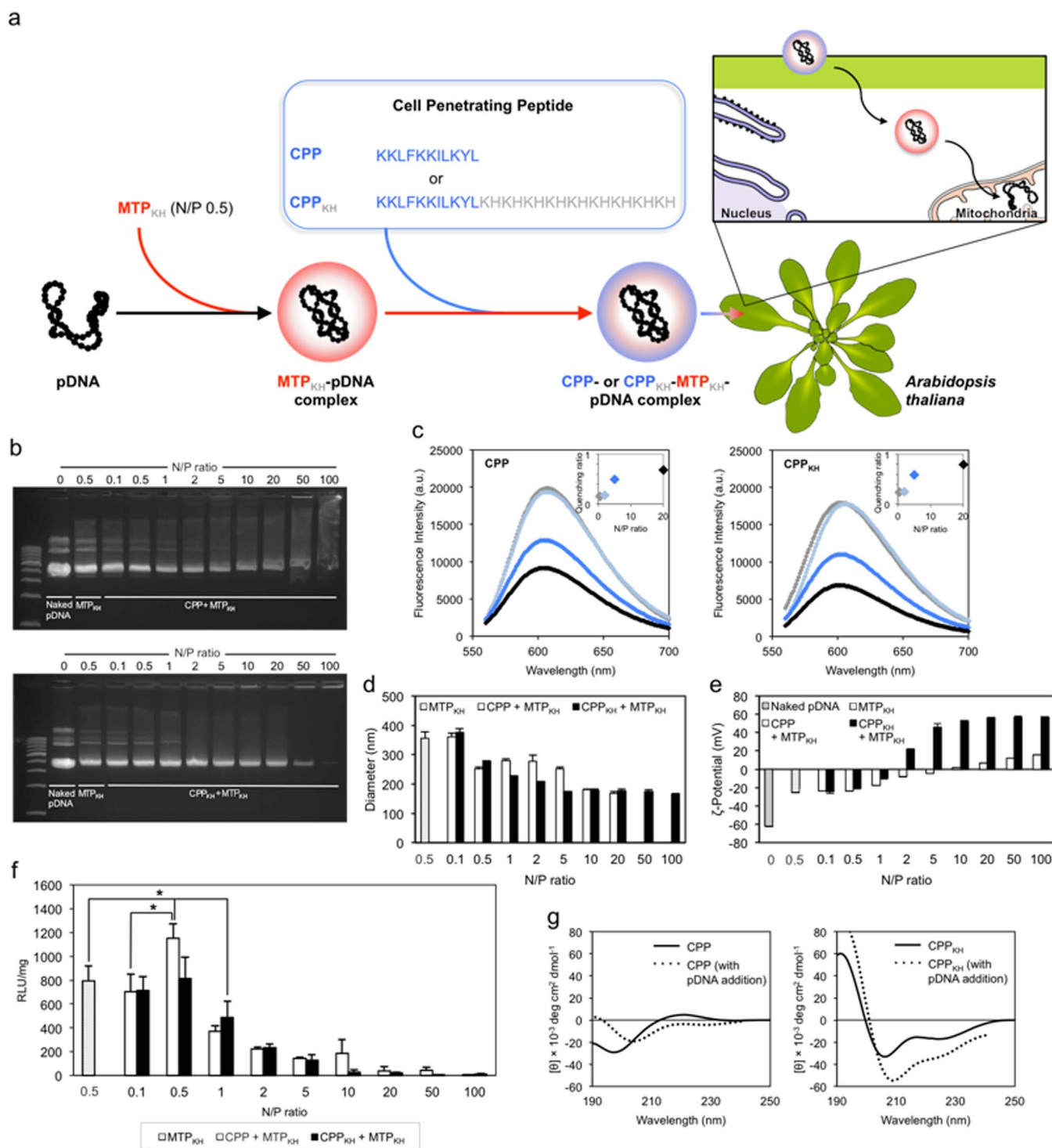


Figure 2 | Combination of mitochondria-targeting peptide and cell-penetrating peptide as vector for delivery of pDNA into the leaves of *A. thaliana* localized to the mitochondria. (a) Schematic representation of the gene delivery strategy using CPP-MTP_{KH} or CPP_{KH}-MTP_{KH}. (b) Electrophoretic mobility of pDNA in CPP- or CPP_{KH}-MTP_{KH}-pDNA complexes. (c) Condensation of pDNA by CPP or CPP_{KH} monitored by the EtBr exclusion assay. The inset shows the quenching ratio as a function of N/P ratio. (d, e) Hydrodynamic size and ζ -potential of CPP- or CPP_{KH}-MTP_{KH}-pDNA complexes measured by DLS. Error bars represent standard deviations ($n = 3$). (f) Efficiency of pDNA delivery by CPP-MTP_{KH} or CPP_{KH}-MTP_{KH} determined using RLuc assay. Asterisks (*) indicate significant differences (Tukey's HSD test; $P < 0.05$). Error bars represent standard deviations ($n = 4$). (g) CD spectra of CPP or CPP_{KH} and respective complexes with pDNA in 40% TFE.

by correlating the physicochemical properties of complexes and their corresponding transfection efficiencies. Clearly, an optimal balance was achieved with the formulation (MTP_{KH}-pDNA at N/P 0.5) in terms of binding strength. MTP_{KH} could interact with pDNA in vitro and subsequently dissociate to release the cargo in vivo, where the

interaction, at the same time, compacted pDNA into a form ideal for its uptake in cells (toroid/doughnut structure proposed in these studies^{22,28}). Although MTP_{KH}, at N/P ratios higher than 0.5, resulted in increasingly stable formulations, a previous report showed that peptides with weak affinity for pDNA favour toroidal compaction²⁹. The

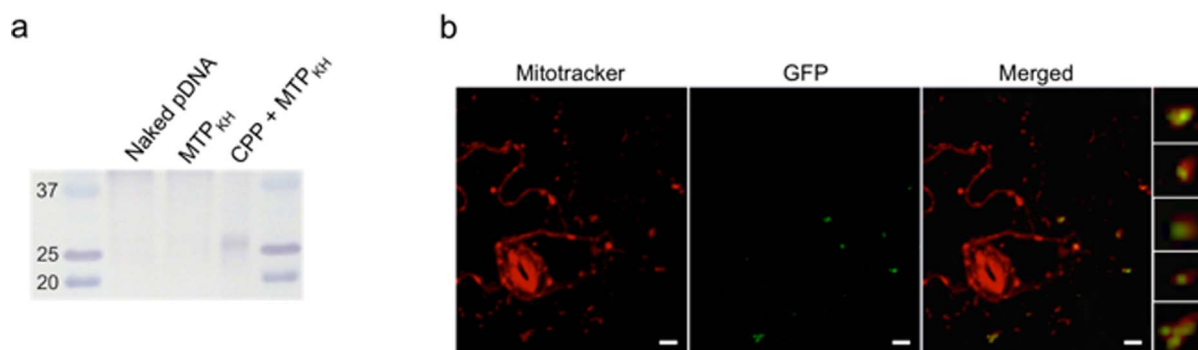


Figure 3 | GFP expression in the mitochondria of *A. thaliana* leaf 12 h after transfection. (a) Western blot analysis of crude mitochondrial extracts from leaves previously infiltrated with naked pDNA, or complexes of MTP_{KH} (N/P 0.5) or CPP-MTP_{KH} (N/P 0.5 for each peptide) with pDNA. Data is representative of two independent experiments. (b) Confocal laser scanning microscope observation of epidermal cells of a leaf previously infiltrated with CPP-MTP_{KH}-pDNA complexes (N/P 0.5 for each peptide). Enlarged images of several mitochondria with GFP expression are shown in the extreme right panel. Scale bars indicate 10 μm .

ability of peptides to aggregate with pDNA, is in fact, highly dependent on peptide structure³⁰ and found to parallel transfection efficiencies¹⁸. Conformational analysis by CD showed that MTP_{KH} was α -helical when bound to pDNA (N/P 0.5). This structural motif is not only essential to the function of mitochondria-targeting peptides^{18,31}, but also allowed topological changes to occur in DNA before charge neutralization point³⁰.

Collectively, our experimental data indicate that MTP_{KH}, even before charge neutralization point (N/P 0.5), could bind/condense pDNA into a size (approximately 350 nm) and structure suited for the endocytic mechanism^{23,24}, and takes a predominant form (α -helical structure) favourable for both cellular³² as well as mitochondrial import³¹. Although, at present, we are unsure of the exact delivery mechanism into the mitochondria by our peptide-based vector, it is possible that the mitochondrial-targeted complex dissociates upon contact with the surface of the mitochondria³³ and the pDNA is imported via the voltage-dependent anion channel followed by the adenine nucleotide translocator⁹. Intracellular penetration was not hindered by the negative surface charge of the complex (approximately -25 mV), which was also the case for other anionic peptide¹⁵ or peptide-pDNA complex¹⁷, suggesting that electrostatic interaction with the cell membrane is not a critical factor for complex internalization.

We then examined the effect of adding cell-penetrating components (CPP or CPP_{KH}) to the MTP_{KH}-pDNA complex. Of note was that CPP and CPP_{KH} share the common ability to decrease the size of MTP_{KH}-pDNA complexes when employed at N/P 0.5 and higher ratios. Modifications in particle size may very well influence gene delivery efficiency as the mechanism of internalization and intracellular routing are known to be size-dependent²⁴. CPP formed only moderately stable particles (15.3 mV) even at the highest N/P ratio while CPP_{KH} formed highly stable particles from N/P 5 to N/P 100 (46.1–57.0 mV) due to an excess of polycations. As ζ -potential is also a measure of colloidal stability²³, particles with strong positive surface charges (i.e. highly stable complexes) will not dissociate easily to release pDNA in vivo, rendering them inefficient gene transfer vehicles.

Although comparable in most aspects (pDNA binding/compactness properties, size and structural propensity), addition of polycations to CPP undeniably altered its properties, justifying the slight discrepancies in performance between CPP and CPP_{KH}. As mentioned previously, helical conformation of cell-penetrating peptides contribute greatly to their internalization³², however, the composition and length of these peptides, as well as the number of cationic residues and even specific positioning of residues in the peptide sequence are equally important factors governing the efficiency of their function¹⁹. Meanwhile, the lesser amount of either CPP or CPP_{KH} (N/P 0.1) failed to improve translocation of more MTP_{KH}-pDNA complexes across the cellular membrane whereas higher con-

centrations of these peptides (N/P 1 to 100) promoted complex stability to a degree that prevented in vivo dissociation, more so in the case of CPP_{KH} with attached polycations.

Overall, the introduction of CPP at N/P 0.5 to preformed MTP_{KH}-pDNA complexes, decreased particle sizes and reduced negative surface charges which ultimately led to a significant boost in transfection levels (a maximum of 1.5-fold increase). The net negative particle surface charge appears to be a persistent feature of our formed complexes, confirming that electrostatic interaction with the cell membrane is indeed not crucial for complex internalization. The negative surface charge may have also contributed positively towards the passage of complexes through the cell wall. Positively-charged complexes could be trapped within the cell wall through the formation of new hydrogen bonds with negatively-charged constituent molecules of the cell wall, thereby reducing the number of complexes that are able to reach the cell membrane.

In this study, we introduced a new and feasible strategy for delivery of genes to the mitochondria of *A. thaliana* which involves a simple combination of cell-penetrating peptide and mitochondria-targeting peptide. A low concentration of each peptide component was sufficient to constitute a carrier that enabled pDNA to be delivered into the cells and targeted to the mitochondria, where the imported pDNA was expressed to detectable levels within a short period of time. Characterization of mitochondria-targeting peptide and cell-penetrating/mitochondria-targeting peptide mediated gene transfer revealed that mitochondrial-targeted pDNA delivery is a function of complexation and induction of cellular uptake but not of electrostatically-driven cell membrane association. While the present study has laid the groundwork for rational design of peptide-based gene carriers, further exploration of peptide sequences are instrumental to improve the success rates of cellular/mitochondrial translocation. As we have demonstrated transfection of intact plant mitochondria, we now look forward to the development of highly competent selection/screening strategies towards the creation of a new and powerful genetic engineering technology that can potentially redefine the boundaries of biological research.

Methods

Peptides. Mitochondria-targeting peptides [MTP, 1525.88 Da; MTP_{KH}, 3913.71 Da] and cell-penetrating peptides [CPP, 1421.88 Da; CPP_{KH}, 3809.71 Da] were synthesized by the Research Resources Center of RIKEN Brain Science Institute.

Plasmid DNA. Plasmids pDONR-cox2:rluc and pDONR-cox2:gfp which contain genes encoding RLuc and GFP, respectively, were constructed according to standard molecular biology protocols³⁴. Yeast cox2 promoter for RLuc gene expression was amplified with Sccox2pFattb1 (5'-GGGGACAAGTTTGTACAAAAAAGCA-GGCTTCTACATCTCCTTCGGCCGGAC-3') and Sccox2pRluc2 (5'-ATCATAAACTTTCGAAGTCATTGTAAATTGTAATCTTAATAAATC-3'). RLuc gene was amplified with RlucF2 (5'-ATGACTTCGAAAGTTTATGATC-3')



and RLucR2attb2 (5'-GGGGACCACTTTGTACAAGAAAGCTGGGTTTTA-TTGTCATTTTTGAGAAC-3'). The resultant fragments were annealed following a denaturation step and the fused PCR products, designated cox2:rluc, served as a template for amplification with Sccox2pFattb1 and RLucR2attb2. In a similar manner, yeast cox2 promoter for GFP expression was amplified with Sccox2pFattb1 and cox2pRGFPs65T (5'-CTCCTCGCCCTTGCTCACCATTGTTAATTGTAATCTT-AATAAATC-3'). GFP s65t was amplified with GFPs65tF (5'-ATGGTGAGCA-AGGGCGAGGAG-3') and GFPs65tRattb2 (5'-GGGGACCACTTTGTA-CAAGAAAGCTGGGTTTTACTTGTACAGCTCGTCCATG-3'). The resultant fragments were annealed following a denaturation step and the fused PCR products, designated cox2:gfp, served as a template for amplification with Sccox2pFattb1 and GFPs65tRattb2. All PCR reactions were performed using KOD-Plus-Ver.2 (TOYOBO CO., LTD., Osaka, Japan). The amplified cox2:rluc and cox2:gfp fragments were subsequently cloned into pDONR207 by BP reaction (Life technology Corp., Carlsbad, CA), resulting in pDONR-cox2p:rluc and pDONR-cox2p:gfp, respectively.

Complex formation. MTP- or MTP_{KH}-pDNA complexes were prepared by adding 2.5 μ L of 1 mg/mL pDNA to increasing volumes of each mitochondria-targeting peptide at various N/P ratios (0.1, 0.5, 1, 2, 5, 10, 20, 50, 100) and autoclaved Milli-Q water to obtain a final volume of 100 μ L. The solution was thoroughly mixed (by repeated pipetting) and allowed to stabilize for 30 min at 25°C. CPP- or CPP_{KH}-MTP_{KH}-pDNA complexes were prepared in a similar manner, by adding increasing volumes of each cell-penetrating peptide at various N/P ratios (0.1, 0.5, 1, 2, 5, 10, 20, 50, 100) to preformed MTP_{KH}-pDNA complexes (N/P 0.5) and autoclaved Milli-Q water to obtain a final volume of 100 μ L. The solution was thoroughly mixed and allowed to stabilize for 30 min at 25°C.

Electrophoretic mobility shift assay, dynamic light scattering and scanning electron microscopy. Assessment of complex stability by electrophoretic mobility shift assay, as well as measurements of particle size and ζ -potential by DLS, were as described previously¹⁷. Complex size and morphology were also investigated by SEM. Samples were mounted on an aluminium stub, sputter coated with gold and examined in the SEM (JSM6330F, JEOL Ltd., Tokyo, Japan) at an accelerating voltage of 5 kV.

Ethidium bromide displacement assay. The degree of pDNA binding/condensation by each peptide was determined by EtBr displacement assay. Before measurement, pDNA (78.8 μ g/mL) was incubated with EtBr (19.7 μ g/mL) for 1 hour. Each peptide was then added to the pDNA-EtBr solution (200 μ L total volume). The emission spectra were recorded from 560 to 700 nm with excitation at 526 nm using Spectra MAX M3 (Molecular Devices Corporation, Sunnyvale, CA). Fluorescence intensity was determined after subtracting the background fluorescence of EtBr in the absence of pDNA.

Circular dichroism spectroscopy. The structure of peptides and conformational changes caused by interaction with pDNA were analysed by CD spectroscopy. Peptides (25 μ M) and their complexes with pDNA (N/P 0.5) were stabilized by the addition of 40% (v/v) 2,2,2-trifluoroethanol (TFE), and the CD spectra were acquired using a Jasco J-820 CD spectropolarimeter. Background scans were obtained for 40% TFE in water. Measurements were made using a quartz cuvette with 0.1 cm pathlength. Each spectra represents the average of three scans from 190 to 250 nm with 0.2 nm resolution. The scans were obtained at 20 nm min⁻¹ with a bandwidth of 1.0 nm and assignments of secondary structures were based on the method of Yang et al²⁷.

Plant growth conditions and transfection with peptide-pDNA complex.

Arabidopsis thaliana, which serves as a model plant system in this study, was grown under the same conditions used previously¹⁷. Leaves were infiltrated with complexes as described¹⁷, and sampled at intermittent time points of 3 h, 6 h, 12 h, 24 h, 36 h and 48 h.

Renilla luciferase assay. Expression of RLuc gene in the mitochondria was evaluated quantitatively by RLuc assay as detailed here¹⁷.

Confocal laser scanning microscopy and Western blot analysis. Expression of GFP gene in the mitochondria was evaluated qualitatively by confocal laser scanning microscopy as detailed here¹⁷. Prior to microscopic observation, mitochondria were stained with MitoTracker Red CMXRos (Molecular Probes, The Netherlands) as follows: leaves were incubated in a 1 μ M dye solution containing phosphate buffered saline (PBS) for 30 min and then washed three times in dye-free PBS to eliminate excess dye. Additionally, GFP expression was detected by Western blot analysis using a suspension of crude mitochondria isolated from leaves previously infiltrated with peptide-pDNA complexes (final pDNA amount of 10 μ g). *A. thaliana* leaf mitochondria was prepared according to an established protocol³⁵ with these modifications: the starting material consisted of 20–30 leaves; 10 mL of grinding buffer A was used; and following the final step, the crude mitochondria suspension was further concentrated by centrifugation and resuspension to an approximate final volume of 50 μ L in wash buffer A. The resultant solution was then separated on a gradient SDS-PAGE gel and transferred to an Invitrolon™ PVDF membrane (Invitrogen, Carlsbad, CA) using a Mini Trans-Blot® SD Semi-Dry Electrophoretic Transfer Cell (Bio-Rad, Hercules, CA). GFP was detected using a mouse monoclonal anti-GFP antibody (1 : 200; ab38689, Abcam) and goat anti-mouse IgG conjugated

with alkaline phosphatase as a secondary antibody (1 : 2000; sc-2008, Santa Cruz Biotechnology).

Statistical analysis. SPSS 17.0 for Windows (IBM, Armonk, NY) was employed for statistical analysis. Tukey's Honestly Significant Difference (HSD) test was used in conjunction with analysis of variance (ANOVA) for single-step multiple comparisons. Differences between two means were considered statistically significant at $P < 0.05$ and indicated with asterisks (*). Data in experiments are expressed as means \pm standard deviation ($n = 3$) for size and ζ -potential measurements, and ($n = 4$) for transfection efficiencies quantified by RLuc assay.

- Jacoby, R. P. *et al.* Mitochondrial composition, function and stress response in plants. *J. Integr. Plant Biol.* **54**, 887–906 (2012).
- Scheffler, I. E. *Mitochondria*, 2nd ed. (John Wiley & Sons, Inc., 2008).
- Mackenzie, S. & McIntosh, L. Higher plant mitochondria. *Plant Cell* **11**, 571–585 (1999).
- Woodson, J. D. & Chory, J. Coordination of gene expression between organellar and nuclear genomes. *Nat. Rev. Genet.* **9**, 383–395 (2008).
- Oksman-Caldentey, K.-M. & Inzé, D. Plant cell factories in the post-genomic era: new ways to produce designer secondary metabolites. *Trends Plant Sci.* **9**, 433–440 (2004).
- Meyers, B., Zaltsman, A., Lacroix, B., Kozlovsky, S. V. & Krichevsky, A. Nuclear and plastid genetic engineering of plants: comparison of opportunities and challenges. *Biotechnol. Adv.* **28**, 747–756 (2010).
- Daniell, H. & Chase, C. *Molecular Biology and Biotechnology of Plant Organelles*. (Springer, Berlin-Heidelberg, 2004).
- Farré, J.-C. & Araya, A. Gene expression in isolated plant mitochondria: high fidelity of transcription, splicing and editing of a transgene product in electroporated organelles. *Nucl. Acids Res.* **29**, 2484–2491 (2001).
- Koulinchenko, M., Konstantinov, Y. & Dietrich, A. Plant mitochondria actively import DNA via the permeability transition pore complex. *EMBO J.* **22**, 1245–1254 (2003).
- Fox, T. D., Sanford, J. C. & McMullin, T. W. Plasmids can stably transform yeast mitochondria lacking endogenous mtDNA. *Proc. Natl. Acad. Sci. USA* **85**, 7288–7292 (1988).
- Johnston, S., Anziano, P., Shark, K., Sanford, J. & Butow, R. Mitochondrial transformation in yeast by bombardment with microprojectiles. *Science* **240**, 1538–1541 (1988).
- Randolph-Anderson, B. L. *et al.* Further characterization of the respiratory deficient dum-1 mutation of *Chlamydomonas reinhardtii* and its use as a recipient for mitochondrial transformation. *Mol. Gen. Genet.* **236**, 235–244 (1993).
- Remacle, C., Cardol, P., Coosemans, N., Gaisne, M. & Bonnefoy, N. High-efficiency biolistic transformation of *Chlamydomonas* mitochondria can be used to insert mutations in complex I genes. *Proc. Natl. Acad. Sci. USA* **103**, 4771–4776 (2006).
- Eggenberger, K., Mink, C., Wadhvani, P., Ulrich, A. S. & Nick, P. Using the peptide Bp100 as a cell-penetrating tool for the chemical engineering of actin filaments within living plant cells. *ChemBioChem* **12**, 132–137 (2011).
- Martin, L., Teixidó, M. & Giral, E. Design, synthesis and characterization of a new anionic cell-penetrating peptide: SAP(E). *ChemBioChem* **12**, 896–903 (2011).
- Chen, Q. R., Zhang, L., Stass, S. A. & Mixson, A. J. Co-polymer of histidine and lysine markedly enhances transfection efficiency of liposomes. *Gene Ther.* **7**, 1698–1705 (2000).
- Lakshmanan, M., Kodama, Y., Yoshizumi, T., Sudesh, K. & Numata, K. Rapid and efficient gene delivery into plant cells using designed peptide carriers. *Biomacromolecules* **14**, 10–16 (2012).
- Niidome, T. *et al.* Binding of cationic α -helical peptides to plasmid DNA and their gene transfer abilities into cells. *J. Biol. Chem.* **272**, 15307–15312 (1997).
- Chugh, A., Eudes, F. & Shim, Y.-S. Cell-penetrating peptides: nanocarrier for macromolecule delivery in living cells. *IUBMB Life* **62**, 183–193 (2010).
- Numata, K., Ohtani, M., Yoshizumi, T., Demura, T. & Kodama, Y. Local gene silencing in plants via synthetic dsRNA and carrier peptide. *Plant Biotechnol. J.* **12**, 1027–1034 (2014).
- Hurt, E. C., Pesold-Hurt, B., Suda, K., Oppliger, W. & Schatz, G. The first twelve amino acids (less than half of the pre-sequence) of an imported mitochondrial protein can direct mouse cytosolic dihydrofolate reductase into the yeast mitochondrial matrix. *EMBO J.* **4**, 2061–2068 (1985).
- Wagner, E., Cotten, M., Foisner, R. & Birnstiel, M. L. Transferrin-polycation-DNA complexes: the effect of polycations on the structure of the complex and DNA delivery to cells. *Proc. Natl. Acad. Sci. USA* **88**, 4255–4259 (1991).
- Adler, A. F. & Leong, K. W. Emerging links between surface nanotechnology and endocytosis: impact on nonviral gene delivery. *Nano Today* **5**, 553–569 (2010).
- Rejmánek, J., Oberle, V., Zuhorn, I. S. & Hoekstra, D. Size-dependent internalization of particles via the pathways of clathrin- and caveolae-mediated endocytosis. *Biochem. J.* **377**, 159–169 (2004).
- Gratton, S. E. A. *et al.* The effect of particle design on cellular internalization pathways. *Proc. Natl. Acad. Sci. USA* **105**, 11613–11618 (2008).
- Mutoh, M. *et al.* Suppression of cyclooxygenase-2 promoter-dependent transcriptional activity in colon cancer cells by chemopreventive agents with a resorcin-type structure. *Carcinogenesis* **21**, 959–963 (2000).



27. Yang, J. T., Wu, C. S. C. & Martinez, H. M. Calculation of protein conformation from circular dichroism. *Methods Enzymol.* **130**, 208–269 (1986).
28. Osada, K. *et al.* Quantized folding of plasmid DNA condensed with block cationomer into characteristic rod structures promoting transgene efficacy. *J. Am. Chem. Soc.* **132**, 12343–12348 (2010).
29. Haley, J., Kabiru, P. & Geng, Y. Effect of clustered peptide binding on DNA condensation. *Mol. BioSyst.* **6**, 249–255 (2010).
30. Dufourcq, J., Neri, W. & N, H.-T. Molecular assembling of DNA with amphipathic peptides. *FEBS Lett.* **421**, 7–11 (1998).
31. Emanuelsson, O., Nielsen, H., Brunak, S. & von Heijne, G. Predicting subcellular localization of proteins based on their N-terminal amino acid sequence. *J. Mol. Biol.* **300**, 1005–1016 (2000).
32. Eiríksdóttir, E., Konate, K., Langel, Ü., Divita, G. & Deshayes, S. Secondary structure of cell-penetrating peptides controls membrane interaction and insertion. *Biochim. Biophys. Acta* **1798**, 1119–1128 (2010).
33. Weissig, V., D'Souza, G. G. M. & Torchilin, V. P. DQAsome/DNA complexes release DNA upon contact with isolated mouse liver mitochondria. *J. Control. Release* **75**, 401–408 (2001).
34. Sambrook, J., Fritsch, E. F. & Maniatis, T. *Molecular Cloning: A Laboratory Manual, 2nd ed.* (Cold Spring Harbor Laboratory Press, Cold Spring Harbor, New York, 1989).
35. Keech, O., Dizengremel, P. & Gardeström, P. Preparation of leaf mitochondria from *Arabidopsis thaliana*. *Physiol. Plant.* **124**, 403–409 (2005).

Acknowledgments

This work was funded by the New Energy and Industrial Technology Development Organization, Japan.

Author contributions

J.C. and K.N. conceived the study and designed the experiments. T.Y. and Y.K. constructed the plasmids. J.C. performed experiments and analysed the data. J.C. wrote and K.N. edited the manuscript.

Additional information

Supplementary information accompanies this paper at <http://www.nature.com/scientificreports>

Competing financial interests: The authors declare no competing financial interests.

How to cite this article: Chuah, J.-A., Yoshizumi, T., Kodama, Y. & Numata, K. Gene introduction into the mitochondria of *Arabidopsis thaliana* via peptide-based carriers. *Sci. Rep.* **5**, 7751; DOI:10.1038/srep07751 (2015).



This work is licensed under a Creative Commons Attribution 4.0 International License. The images or other third party material in this article are included in the article's Creative Commons license, unless indicated otherwise in the credit line; if the material is not included under the Creative Commons license, users will need to obtain permission from the license holder in order to reproduce the material. To view a copy of this license, visit <http://creativecommons.org/licenses/by/4.0/>